



# Microstructural evolution of Alloy 718 at high helium and hydrogen generation rates during irradiation with 600–800 MeV protons

B.H. Sencer<sup>a,b,\*</sup>, G.M. Bond<sup>a</sup>, F.A. Garner<sup>b</sup>, M.L. Hamilton<sup>b</sup>, B.M. Oliver<sup>b</sup>,  
L.E. Thomas<sup>b</sup>, S.A. Maloy<sup>c</sup>, W.F. Sommer<sup>c</sup>, M.R. James<sup>c</sup>, P.D. Ferguson<sup>c</sup>

<sup>a</sup> *New Mexico Tech, Socorro, NM, USA*

<sup>b</sup> *Materials Research Department, Pacific Northwest National Laboratory, P.O. Box 999, Building #326, Battelle Boulevard, P8-15, Richland, WA 99352, USA*

<sup>c</sup> *Los Alamos National Laboratory, Los Alamos, NM, USA*

## Abstract

When precipitation hardened Alloy 718 is irradiated with high-energy protons (600–800 MeV) and spallation neutrons at temperatures below  $\sim 60^\circ\text{C}$ , it quickly hardens and loses almost all uniform elongation. It later softens somewhat at higher exposures but does not regain any elongation. This behavior is explained in terms of the evolution of Frank loop formation, disordering and eventual dissolution of the  $\gamma'$  and  $\gamma''$  strengthening phases, and the steady accumulation of very large levels of helium and hydrogen. These gases must be dispersed on a very fine scale in the matrix since no cavities could be found. © 2000 Elsevier Science B.V. All rights reserved.

## 1. Introduction

In both fusion neutron spectra and in the mixed proton–spallation neutron spectra generated in accelerator-driven spallation systems, the displacement damage in typical structural alloys is accompanied by very large generation rates of both helium and hydrogen. While helium is generally thought to be an embrittlement problem mostly for higher-temperature applications, hydrogen is usually thought to exert its influence on embrittlement most strongly at lower temperatures, especially when there are high densities of radiation-induced defects available for trapping, and when large amounts of helium are being generated concurrently [1,2].

There is currently a proposal to use an accelerator-driven system to serve as a fusion-relevant irradiation facility [3]. The proposed source (target) in this facility would consist of tungsten rods clad with Alloy 718, a

concept already successfully demonstrated in the accelerator production of tritium (APT) program [4]. The cladding of such rods typically experiences temperatures up to  $200^\circ\text{C}$ .

Data recently obtained from the APT program on the changes in mechanical properties of Alloy 718 under irradiation are potentially useful to the fusion community. Hamilton et al. [5] have shown that irradiation of Alloy 718 with a mixed spectrum of protons and spallation neutrons, causes the alloy to harden very quickly at irradiation temperatures  $<60^\circ\text{C}$ . The alloy loses most of its uniform elongation before 0.5 dpa is attained, as shown in Fig. 1. There is a tendency for the alloy to soften somewhat with increased irradiation dose, but there is no concurrent recovery in the tensile uniform elongation.

During irradiation in the Los Alamos Spallation Radiation Effects Facility, helium is being generated in Alloy 718 at a rate of  $\sim 150$  appm/dpa, and hydrogen at a rate that is approximately 10 times higher, but about one-half of the hydrogen is lost by energetic recoil and additional losses occur by diffusion [6]. Alloy 718 initially increases in hydrogen content at a high rate and has retained  $\sim 2800$  appm hydrogen at  $\sim 4$  dpa,

\* Corresponding author. Tel.: +1-509 376 0156; fax: +1-509 376 0418.

E-mail address: bulent.sencer@pnl.gov (B.H. Sencer).

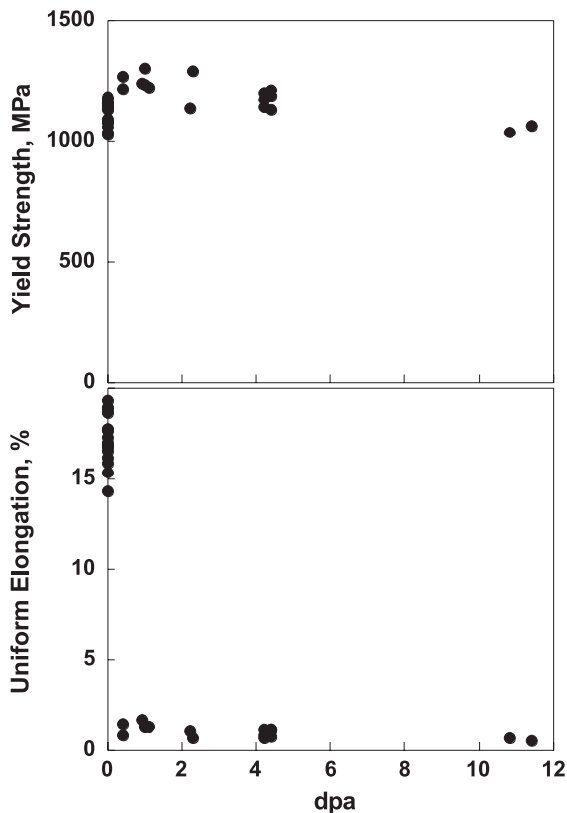


Fig. 1. Effect of dose on yield strength and uniform elongation of Alloy 718 irradiated with high-energy protons and spallation neutrons, with irradiation temperatures of 32–55°C and test temperatures <60°C [5].

indicating that a significant fraction of the hydrogen has been retained. As the dpa level increases beyond 4 dpa, hydrogen is retained at a somewhat lower rate, reaching ~5000 appm hydrogen at 10–13 dpa.

In order to determine the microstructural origins of the observed changes in mechanical properties, Alloy 718 specimens irradiated at doses ranging between ~0.5 and ~13 dpa were examined by transmission electron microscopy (TEM).

## 2. Experimental details

Alloy 718 is a  $\gamma'$ - $\gamma''$  age-hardenable superalloy containing Nb, Ta, Mo, Ti, and Al. The heat of material used in this study had the following composition: 53.58%Ni, 18.37%Fe, 18.13%Cr, 4.98%(Nb + Ta), 3.06%Mo, 1.03%Ti, 0.11%Si, 0.48%Al, 0.13%Mn, 0.08%Cu, 0.04%C, 0.001%S, 0.008%P (in wt%). Specimens examined in this study were prepared by EDM and cut in the form of standard 3-mm TEM disks. These

were heat treated at 1065°C /30 min, air cooled room temperature then aged at 760°C for 10 h, furnace cooled to 650°C for a total time of 20 h, and air cooled to room temperature.

The irradiation was conducted in the Los Alamos Spallation Radiation Effects Facility at Los Alamos National Laboratory. Details of the irradiation experiment were published previously [4]. In this specimen series there was a Gaussian proton flux having a circular profile in intensity of 2 sigma = 3 cm over the specimen ensemble.

The proton energy varied from the incident energy of 800 MeV down to ~600 MeV, and there were also spallation neutrons over a wide range of energies at fluxes an order of magnitude lower than that of the protons [6]. Six irradiated specimens were chosen for TEM analysis depending on the proton beam intensity at their locations. The irradiation temperature varied somewhat with dose rate, such that the temperature was ~32°C at the lowest dose, 0.6 dpa, and ~55°C at 13.4 dpa.

Thin foil samples were prepared for TEM examination by conventional jet electropolishing methods, in 5% perchloric acid, 95% ethyl alcohol at -25°C and 55 V. TEM examinations were conducted with JEOL 2010F FEG-STEM, JEOL 2000E and JEOL 1200EX electron microscopes.

## 3. Results

### 3.1. TEM characterization of unirradiated Alloy 718

The microstructure of the unirradiated Alloy 718 was found to contain spheroidal  $\gamma'$  and disc-shaped  $\gamma''$  precipitates with sizes in the range of 10–26 and 12–47 nm, respectively. The  $\gamma'$  and  $\gamma''$  phases represent ordered variations of the fcc lattice.  $\gamma'$  has a cubic  $L1_2$  ordered structure based on  $Ni_3(Ti,Al)$ .  $\gamma''$  has a tetragonal  $DO_{22}$  ordered structure based on  $Ni_3Nb$  [7]. Also observed were inhomogeneously dispersed inclusions, and extensive thermal twinning. TEM-EDS analysis was performed to identify some inclusions that were observed. The inclusions were shown to be Nb-rich carbides with an average composition between (80–86)%Nb, (7–11)%Ti, and small amounts of Mo, Ni, Cr, and Fe. No overaging phases such as  $\eta$  were observed in the austenitic  $\gamma$  matrix. In the [001] lattice image shown in Fig. 2 the  $\gamma'$  is distinguished from the fcc matrix by its doubled lattice spacing. In addition, lattice imaging of unirradiated 718 revealed that the intragranular  $\gamma'$  and  $\gamma''$  particles usually occur in pairs, each  $\gamma''$  particle sharing an interface with a  $\gamma'$  particle and showing evidence of coherency strain along its interface with the matrix.

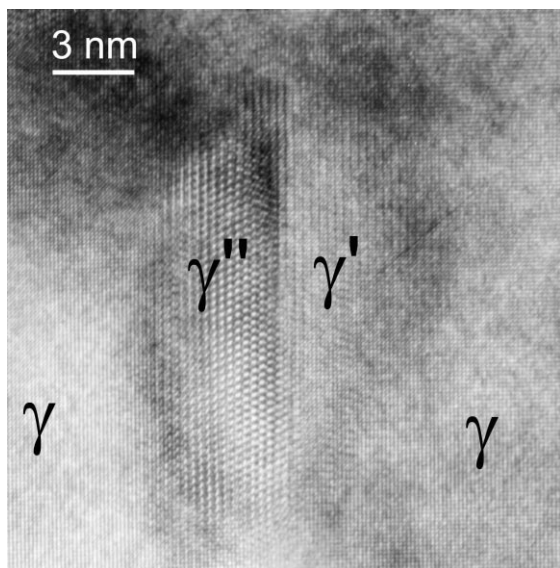


Fig. 2. High-resolution electron micrograph of  $\gamma'$ - $\gamma''$  structures in unirradiated Alloy 718. [001] lattice image.

### 3.2. TEM characterization of irradiated Alloy 718

**Phase stability.** Under mixed proton and spallation neutron irradiation, the  $\gamma'$  and  $\gamma''$  phases seem to have disappeared at doses as low as 0.6 dpa. As shown by Fig. 3, the  $\gamma''$  and  $\gamma''$  superlattice diffraction spots observed in the unirradiated samples were absent after irradiation. The Nb-rich carbides were still present, however, and were still crystalline after irradiation.

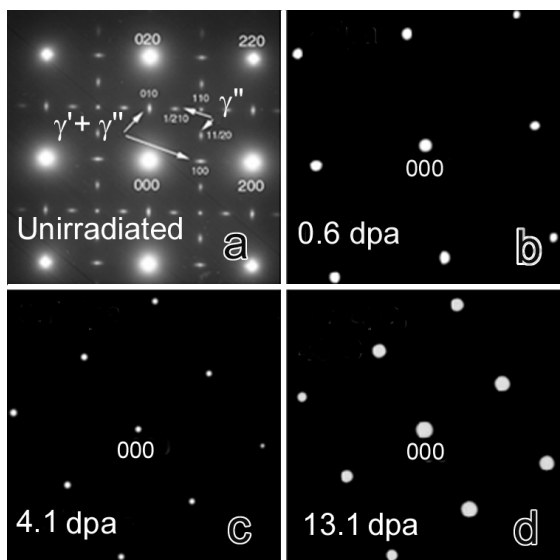


Fig. 3. [001] Selected-area electron diffraction patterns from Alloy 718: (a) showing  $\gamma'$  and  $\gamma''$  reflections, (b),(c),(d) showing disappearance of  $\gamma'$  and  $\gamma''$  reflections after irradiation.

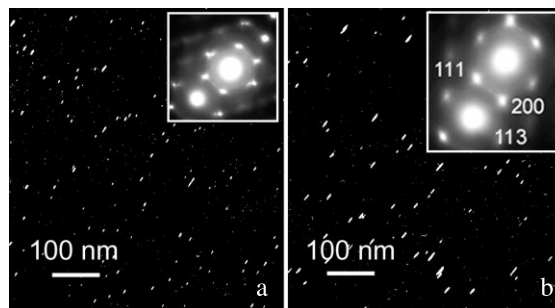


Fig. 4. Faulted Frank loops, in (a) 3.8 and (b) 13.4 dpa samples, imaged with one of the  $\langle 111 \rangle$  relrods. Corresponding diffraction patterns are shown as insets.

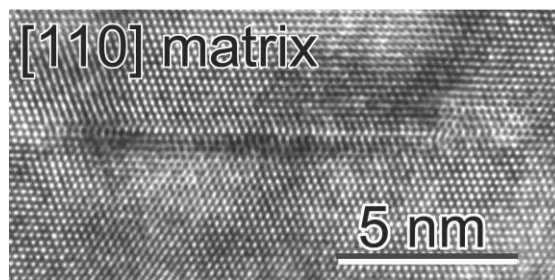


Fig. 5. High-resolution electron micrograph of radiation-induced Frank loop near edge-on in irradiated Alloy 718, 1.5 dpa. [011] lattice image.

**Radiation-induced defects.**  $\{111\}$ -faulted Frank dislocation loops were observed at all dpa levels. The loops produced distinctive satellite spots around the fundamental matrix diffraction spots. The satellite spots arise from extended diffraction streaks (relrods) perpendicular to the four sets of  $\{111\}$  planes. Essentially identical intensities of satellite diffraction spots from the four  $\langle 111 \rangle$  relrods indicated similar Frank-loop populations on all four  $\{111\}$  planes. The Frank loops were imaged with a  $\langle 111 \rangle$  relrod in specimens at 3.8 and 13.4 dpa, as shown in Fig. 4. Fig. 5 also shows the high-resolution [011] lattice image of an edge-on Frank loop at 1.5 dpa. Small (black-spot-damage) and larger faulted Frank loops were visible in all samples, and they increased in size with increasing dose.

The possibility of cavity formation was investigated in Fresnel contrast. This technique enables the detection of cavities as small as 1 nm [8]. However, no cavity (bubble and/or void) formation was found in the samples examined between 0.6 and 13.4 dpa (Fig. 6).

## 4. Discussion

A very significant observation is the absence of any type of cavity, even though levels of  $\sim 1830$  appm helium

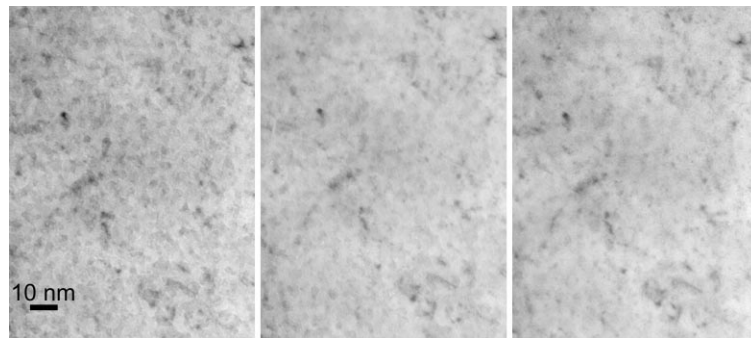


Fig. 6. Kinematic through-focal image series from 13.4 dpa Alloy 718. From left to right: under-focus, focus and over-focus, showing that no cavities are observed in the matrix.

and  $\sim 5000$  appm hydrogen were reached at 13.4 dpa. In the irradiation temperature range 32–55°C, it appears that there is insufficient mobility of helium atoms to allow nucleation and growth of bubbles or voids.

The disappearance of the  $\gamma'$  and  $\gamma''$  precipitates at a dose well below  $\sim 1$  dpa is also thought to be very significant. This is somewhat different from the behavior observed in Inconel 718 at a somewhat higher temperature,  $\sim 288^\circ\text{C}$ , in a boiling-water reactor (BWR). Both the disappearance of  $\gamma''$  and redistribution of  $\gamma'$  were reported [9]. In the BWR study  $\gamma''$  disappeared after doses of between 2.5 and 3.5 dpa. After doses of 2.5–6 dpa, the original  $\gamma'$  particles were visible, but just breaking into smaller discrete particles. After 20 dpa, only a few of the original  $\gamma'$  particles were still visible, and the matrix contained finer dispersed  $\gamma'$  particles. The redistribution indicates that a new balance between dissolution and thermally induced diffusion has occurred at this higher temperature. Carsughi et al. [10] also observed the disappearance of  $\gamma'$  and  $\gamma''$  in Inconel 718 after irradiation with 800 MeV protons to  $\sim 10$  dpa at temperatures below 250°C.

At low irradiation temperatures, thermal diffusion is very limited and cascade-induced mixing can become the most important short-range transport mechanism. Under 600–800 MeV proton irradiation, very large cascades are thought to be produced. At only a level of 0.6 dpa, it is difficult to see how complete dissolution of these precipitates and redistribution of the contained solutes could occur. It is thought to be more likely that mixing-induced disordering of the  $\gamma'$  and  $\gamma''$  occurs initially, leading to the rapid loss of order-induced imaging in the microscope, but not the immediate dispersion of the concentrated solutes that comprise the precipitates. Redistribution of the solutes is then thought to follow as the dose increases. This scenario is consistent with the dose scale on which the various changes were observed in the yield strength. Complete dissolution by 0.6 dpa would lead to a softening that is inconsistent with the initial hardening observed. This scenario will be tested

by future examination of specimens irradiated to  $< 0.1$  dpa, where it is hoped that the disordering may be captured in progress [11].

If we assume that the now-disordered precipitates are still present and thereby retain most of their hardening capability, as solute-rich regions in the matrix, then the formation of a high density of black spot damage and Frank loops is obviously responsible for the initial increase in strength. At 0.6 dpa the gas generation is thought to be insufficient to account for the initial hardening. The later partial softening is thought to result from a more complete mixing-induced redistribution of the solutes comprising the precipitates. A loss of strength is usually accompanied by an increase in ductility, but mechanical testing has shown a dramatic drop in total elongation occurring prior to  $\sim 0.6$  dpa. This loss is not recovered at higher doses where partial softening occurs. This behavior may be the result of the increasing accumulation of helium and especially hydrogen with increasing dose.

## 5. Conclusions

After irradiation at 32–55°C and doses ranging from 0.6 to 13.4 dpa, precipitation hardened Inconel 718 irradiated with a mixed spectra of high-energy protons and spallation neutrons first hardens at  $< 1$  dpa and then softens slightly at higher dpa levels. The initial hardening is accompanied by a near-total loss of uniform elongation that is not recovered when the alloy later softens.

Characterization of the microstructure has revealed marked irradiation-induced changes. A wide range of both small and large faulted Frank loops is formed, providing a contribution to hardening. Based on diffraction evidence, both the  $\gamma'$  and  $\gamma''$  precipitates have apparently disappeared by 0.6 dpa, which should lead to softening. It is postulated that the precipitates initially are only disordered at 0.6 dpa but that the solutes they

contained are not fully redistributed back into the matrix. Thus, the precipitates retain the majority of their original hardening contribution while effectively disappearing from view. The subsequent softening is thought to be associated with more effective redistribution of the solutes at higher doses.

In spite of large levels of retained helium and hydrogen, no cavities were found even at the highest doses. These gases are therefore, dispersed on a very fine scale, and this may account for the fact that the initial strong loss of uniform elongation is not partially recovered when the alloy later softens.

### Acknowledgements

This work was supported by the Accelerator Production of Tritium Project and the Office of Fusion Energy Sciences, US Department of Energy under Contract DE-AC06-76RLO 1830.

### References

- [1] F.A. Garner, L.R. Greenwood, *Radiat. Eff. Def. Solids* 144 (1998) 251.
- [2] L.R. Greenwood, F.A. Garner, *J. Nucl. Mater.* 233–237 (1996) 1530.
- [3] W.F. Sommer, P. Ferguson, M. Louthan, R. Johnson, F.A. Garner, Evaluation of a spallation neutron source for fusion-relevant radiation damage effects studies, presented at 9th Int. Conf. on Fusion Reactor Materials (ICFRM-9), Colorado Springs, CO, Oct. 1999.
- [4] S.A. Maloy, W.F. Sommer, R.D. Brown, J.E. Roberts, J. Eddleman, E. Zimmerman, G. Willcutt, in: M.S. Wechler, L.K. Mansur, C.L. Snead, W.F. Sommer (Eds.), *Proceedings of the Symposium on Materials for Spallation Neutron Sources*, TMS, Warrendale, PA, 1998, p. 35.
- [5] M.L. Hamilton, F.A. Garner, M.B. Toloczko, S.A. Maloy, W.F. Sommer, M.R. James, P.D. Ferguson, M.R. Louthan Jr., Shear punch and tensile measurements of mechanical property changes induced in various steels by high energy mixed proton and neutron irradiation at low temperatures, in these proceedings.
- [6] B.M. Oliver, F.A. Garner, S.A. Maloy, W.F. Sommer, M.R. James, P.D. Ferguson, Retention of very high levels of hydrogen generated in various structural alloys by 800 MeV protons and spallation neutrons, in: *Proceedings of the 20th International Symposium on Effects of Radiation on Materials*, ASTM STP 1405, 6–8 June 2000, in press.
- [7] D.F. Paulonis, J.M. Oblak, D.S. Duvall, *Trans. ASM* 62 (1969) 611.
- [8] M. Ruhle, M. Wilkens, *Cryst. Lattice Defects* 6 (1975) 129.
- [9] L.E. Thomas, S.M. Bruemmer, Radiation-induced microstructural evolution and phase stability in nickel-base Alloy 718, in: *Proceedings of the Eighth International Symposium on Environmental Degradation of Materials in Nuclear Power Systems – Water Reactors*, vol. 2, TMS, 1997, pp. 772–779.
- [10] F. Carsughi, H. Derz, P. Ferguson, G. Pott, W. Sommer, H. Ullmaier, *J. Nucl. Mater.* 264 (1999) 78.
- [11] B.H. Sencer, G.M. Bond, F.A. Garner, S.A. Maloy, W.F. Sommer, M.R. James, Microstructural alteration of structural alloys by low temperature irradiation with high energy protons and spallation neutrons, in: *Proceedings of the 20th International Symposium on Effects of Radiation on Materials*, ASTM STP 1405, 6–8 June 2000, in press.